Open access • Journal Article • DOI:10.1049/EL:20000973

Design of photonic crystal optical waveguides with singlemode propagation in the photonic bandgap — Source link

Ali Adibi, Reginald K. Lee, Yong Xu, Amnon Yariv ...+1 more authors

Institutions: California Institute of Technology

Published on: 03 Aug 2000 - Electronics Letters (IET)

Topics: Yablonovite, Photonic crystal, Microstructured optical fiber, Photonics and Nanophotonics

concentration of the substrate was $N_D \sim 10^{15}$cm^{-3} (bulk resistivity $\rho \sim 7.5\Omega$.cm) and the sizes of the heavily doped n^+-regions are $20 \times 150\mu m^2$ (on the mask). The distances of $l_{C1,2}$ and l_{EC1} were 120 and 20μm, respectively. The experiments were carried out at T = 300 and 77K in the range of magnetic fields $1.2T \leq \mathbf{B} \leq 1.2T$.

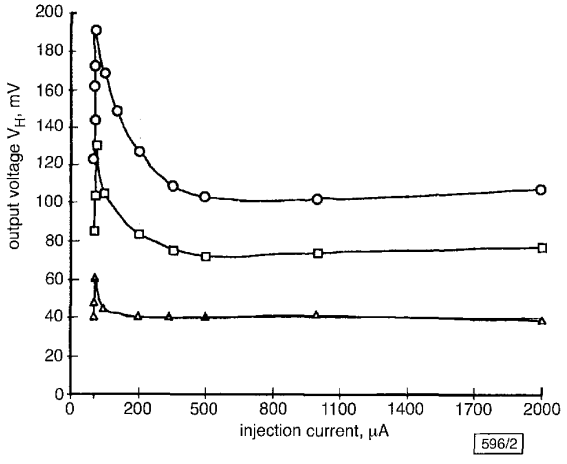

Fig. 2 *Hall voltage V_H against emitter injection I_{EC1} for various bias currents $I_{C1,2}$ at fixed induction $B = 1T$*

△—△ 5mA
□—□ 10mA
○—○ 15mA

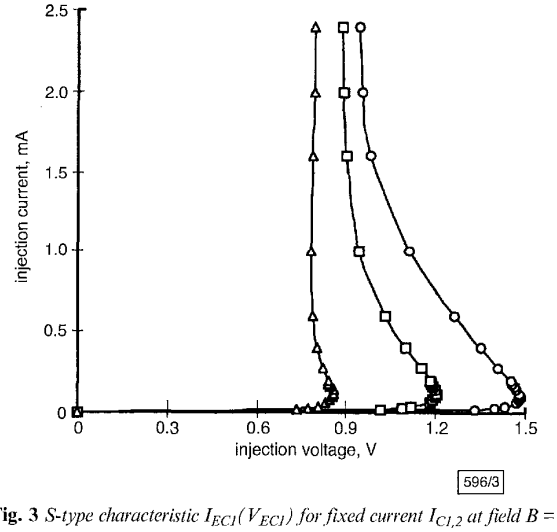

Fig. 3 *S-type characteristic $I_{EC1}(V_{EC1})$ for fixed current $I_{C1,2}$ at field $B = 0$*

Fig. 2 shows the dependencies of the Hall voltage as a function of emitter injection, and Fig. 3 shows the curve $I_{EC1}(V_{EC1})$ at $I_{C1,2} > 0$. The unexpected positive result is that the Hall voltage V_H increases dramatically by ~55% at extremely low emitter current values of 5μA (Fig. 2), i.e. at these injection values, negative resistance occurs (Fig. 3) and a current filament arises at the same time. The nonlinearity NL of the output $V_H(\mathbf{B})$ in the range $-1T \leq \mathbf{B} \leq 1T$ does not exceed the value of NL ≤ 1%, and the temperature coefficient (TC) of the magnetosensitivity TC in the interval $260K \leq T \leq 380K$ becomes TC = 0.1%/K.

The dependencies shown in Figs. 2 and 3 were also recorded at temperature T = 77K on the same samples when their resistance was reduced several times by the increased carrier mobility. It was established that there was no negative resistance over the curve $I_{EC1}(V_{EC1})$ at current $I_{C1,2} > 0$ and that the Hall voltage is practically uninfluenced by the emitter injection.

The obtained results are in complete agreement with the proposed model and are the first evidence in sensor electronics that the sensitivity of a Hall microsensor can be enhanced by minority carrier injection.

3 May 2000
Electronics Letters Online No: 20001017
DOI: 10.1049/el:20001017

Ch.S. Roumenin, D. Nikolov and A. Ivanov (*Institute of Control and System Research, Bulgarian Academy of Sciences, Sofia 1113, PO Box 79, Republic of Bulgaria*)

E-mail: roumenin@bas.bg

References

1 ROUMENIN, Ch.S., and KOSTOV, P.T.: 'Hall effect sensor'. Bulg. Patent 37208, 26 Dec. 1983
2 MAENAKA, K., OHGUSU, T., ISHIDA, M., and NAKAMURA, T.: 'Novel vertical Hall cells in standard bipolar technology', *Electron. Lett.*, 1987, **23**, pp. 1104–1105
3 NAKAMURA, T., and MAENAKA, K.: 'Integrated magnetic sensors', *Sens. Actuators A*, 1990, **21–23**, pp. 762–769
4 ROUMENIN, Ch.S.: 'Solid state magnetic sensors' (Elsevier, Amsterdam, 1994)
5 GILBERT, B.: 'Novel magnetic-field sensor using carrier-domain rotation: proposed device design', *Electron. Lett.*, 1976, **12**, pp. 608–610

Design of photonic crystal optical waveguides with singlemode propagation in the photonic bandgap

A. Adibi, R.K. Lee, Y. Xu, A. Yariv and A. Scherer

The authors present a systematic method for designing dielectric-core photonic crystal optical waveguides that support only one mode in the photonic bandgap (PBG). It is shown that by changing the sizes of the air columns (without perturbing the positions of the centres of the air column) in the two rows that are adjacent to the middle slab, the higher order mode(s) can be pushed out of the photonic bandgap, resulting in singlemode wave propagation in the bandgap.

Photonic crystals have inspired a significant amount of interest recently due to their potential for controlling the propagation of light. Photonic crystals with line defects can be used for guiding light. Guiding light through sharp bends has been recently proposed [1] and demonstrated at optical frequencies [2]. Dielectric-core photonic crystal waveguides are typically generated by removing one row of air holes. This may result in a multimode waveguide that is not suitable for many practical applications. We recently studied the design of a singlemode dielectric-core photonic crystal waveguide by placing a thin dielectric slab between two PBG mirrors. However, the design of bends using such waveguides is complicated due to the breakdown of lattice symmetry. In this Letter, we present a systematic method for designing dielectric-core photonic crystal waveguides that support only one mode in the photonic bandgap (PBG). We show that by changing the sizes of the air columns in the two rows that are adjacent to the middle slab (without perturbing the positions of the centres of the air columns), we can push the higher order mode(s) out of the photonic bandgap. Since we do not change the positions of the centres of the air columns, we can design bends similar to the bends in the multimode waveguides.

The planar PBG waveguide we analyse throughout this Letter is made by removing one row of air columns from a triangular lattice of air columns in silicon (Si). The ratio between the radius of an air column (r) and the lattice period in the horizontal direction (a) is r/a = 0.3. Fig. 1 shows the dispersion diagrams of the TM modes (magnetic field perpendicular to the computation plane) of the PBG waveguide. To analyse the guiding structures, we used a computer code based on the two-dimensional finite difference time domain (2D-FDTD) method [3]. To calculate the dispersion diagram, we used an order-N spectral method [4] in the computational domain shown in Fig. 3a with Bloch boundary conditions on the left and right sides and perfectly matched layers (PML) [5] on the top and bottom of the structure. Throughout this Letter, we assume a = 24 calculation cells.

Fig. 1 shows that there are two modes in the photonic bandgap (PBG). Calculation of the field patterns shows that these two modes have different symmetries (even and odd). This is not desirable for designing practical bends with good transmissivity in the PBG. One idea for obtaining singlemode propagation in the PBG is to reduce the thickness of the middle dielectric slab of the PBG waveguide by increasing the radii of the air columns in the two rows that are adjacent to the middle slab. This results in the higher frequency of both modes, especially the odd mode. This effect is similar to the known property in the conventional dielectric slab waveguides that the dispersion diagram of each guiding mode is shifted upward (towards higher frequencies) by decreasing the slab thickness (or extending the air region).

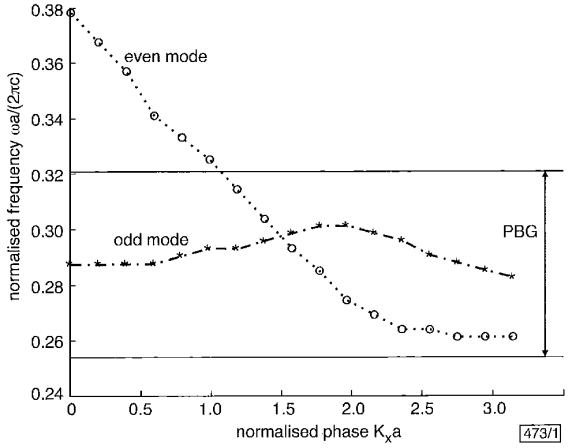

Fig. 1 *Dispersion diagrams of even and odd TM modes (magnetic field normal to calculation plane) for optical waveguide made by removing one row of air columns from two-dimensional photonic crystal consisting of triangular lattice of air columns in silicon (Si)*

Distance between the centres of two adjacent air columns in horizontal direction is a, and radius of an air column is $r = 0.3a$. To take the finite size of the waveguide in the third dimension (perpendicular to calculation plane), we assumed an effective permittivity of $\varepsilon = 7.9$ for Si. The photonic bandgap (PBG) of the photonic crystal ($0.254 < \omega a/(2\pi c) < 0.321$) is also shown

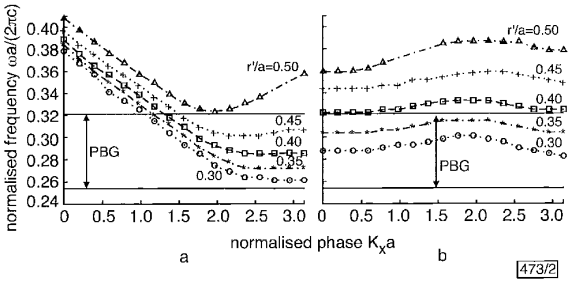

Fig. 2 *Dispersion diagrams of even and odd TM modes of PBG waveguide for different radii (r') of air columns in two rows adjacent to middle slab*

a Even
b Odd
Radii of all other air columns are equal to $r = 0.30a$. The reason for some missing points in these dispersion diagrams is the lossy (low Q) nature of corresponding mode at those points which results into large (> 3%) uncertainty in calculation of frequency of mode

Figs. 2*a* and *b* show the dispersion diagrams of the even and odd modes, respectively, for different radii of the air columns in the two rows adjacent to the middle slab (r'). The radii of all other air columns are $r = 0.30a$ in all cases. Fig. 2*b* shows that for $r'/a > 0.40$ the odd mode is pushed out of the photonic bandgap, while the even mode still covers a considerable portion of the bandgap (except for $r'/a \simeq 0.50$). Therefore, we can obtain singlemode guiding in the PBG by choosing $r'/a > 0.40$. However, choosing r too large results in the excessive upward shift of the even mode reducing the frequency range for singlemode propagation in the PBG. Therefore, the optimum value of r'/a is about 0.40. Fig. 3 shows the patterns of the magnetic field of the odd TM mode at $K_xa = 3\pi/4$ for different values of r'/a. The field patterns at $r'/a = 0.45$ and $r'/a = 0.50$ (Figs. 3*c* and *d*, respectively) show that the odd mode is out of the PBG at these values of r'/a, since the field is extended to the surrounding photonic crystal regions. This is in agreement with the dispersion diagrams of the odd mode at these values of r'/a shown in Fig. 2*b*. The low loss of the optical mode of the waveguide with $r'/a = 0.40$ (even though the mode frequency $\omega a/(2\pi c) = 0.330$ is slightly out of the bandgap) is due to the absence of the photonic crystal modes at that frequency. Note that $0.254 < \omega a/(2\pi c) < 0.321$ represents the absolute bandgap of the photonic crystal. The bandgap (frequency range with no mode present) at a specific value of K_xa can be wider than the absolute bandgap.

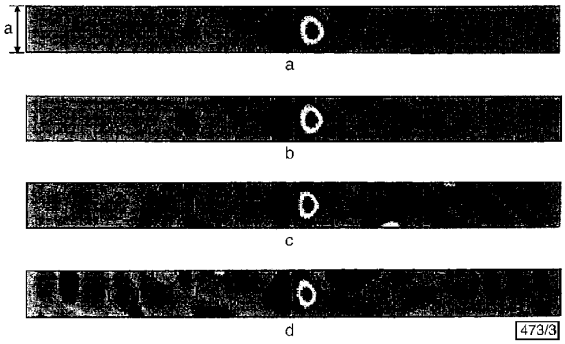

Fig. 3 *Magnetic field (B) patterns of odd TM mode of PBG waveguide at normalised phase*

($K_xa = 3\pi/4$)
a $r' = 0.35a$ and $\omega a/(2\pi c) = 0.311$
b $r' = 0.40a$ and $\omega a/(2\pi c) = 0.330$
c $r' = 0.45a$ and $\omega a/(2\pi c) = 0.359$
d $r' = 0.50a$ and $\omega a/(2\pi c) = 0.416$
In all four cases, $r = 0.30a$
The photonic bandgap is $0.254 < \omega a/(2\pi c) < 0.321$

One interesting property of the even mode is the relatively flat behaviour of the dispersion diagram at higher values of K_xa. This is due to the coupling of the even mode to the other modes of the structure. This coupling is stronger for thinner slabs (or larger r'/a) due to reduced mode confinement in the middle slab. Therefore, the flat region of the even mode is extended to lower values of K_xa by increasing r'/a.

Note that the design of a bend using the proposed waveguide (with singlemode propagation in the PBG) is similar to that using a waveguide made by removing one row of air columns (the waveguide with $r'/a = r/a = 0.3$). The design of the latter has been done by several research groups [1, 2]. The reason for the similarity of the design in two cases is that the positions of the centres of all air columns (including the ones adjacent to the middle slab) are the same in both cases. This is a main advantage of our design.

To summarise, we have presented a systematic way of designing dielectric-core photonic crystal waveguides with only one mode in the photonic bandgap. We showed that by redesigning the two rows of air columns that are adjacent to the middle slab, we can push the higher order mode(s) out of the photonic bandgap.

Acknowledgments: This work was supported in part by the Air Force Office of Scientific Research under contract AFOSR-61557, and by the Office of Naval Research (Y.S. Park).

9 June 2000
Electronics Letters Online No: 20000973
DOI: 10.1049/el:20000973

A. Adibi, R.K. Lee, Y. Xu, A. Yariv and A. Scherer (*California Institute of Technology, Departments of Electrical Engineering and Applied Physics, Pasadena, California 91125, USA*)

A. Adibi: Currently at Georgia Institute of Technology, School of Electrical and Computer Engineering, Atlanta, GA 30332, USA

E-mail: ali.adibi@ece.gatech.edu

References

1 MEKIS, A., CHEN, J.C., KURLAND, I., FAN, S., VILLENEUVE, P.R., and JOANNOPOULOS, J.D.: 'High transmission through sharp bends in photonic crystal waveguides', *Phys. Rev. Lett.*, 1996, **77**, pp. 3787–3790

2 BABA, T., FUKAYA, N., and YONEKURA, J.: 'Observation of light propagation in photonic crystal optical waveguides with bends', *Electron. Lett.*, 1999, **35**, pp. 654–655
3 YEE, K.S.: 'Numerical solution of initial boundary value problems involving Maxwell's equations in isotropic media', *IEEE Trans. Antennas Propag.*, 1966, **AP-14**, pp. 302–307
4 CHAN, C.T., YU, Q.L., and HO, K.M.: 'Order-N spectral method for electromagnetic waves', *Phys Rev B*, 1995, **51**, pp. 16635–16642
5 BERENGER, J.P.: 'A perfectly matched layer for the absorption of electromagnetic waves', *J. Comput. Phys.*, 1994, **114**, pp. 185–200

Narrow-band light emission in semiconductor-fibre asymmetric waveguide coupler

E. Mao, D.R. Yankelevich, C.-C. Lin, O. Solgaard, A. Knoesen and J.S. Harris Jr

A narrow-band, fibre-coupled light emitter based on the evanescent coupling between a semiconductor waveguide and a singlemode fibre is presented. The wavelength selectivity of the emission spectrum is caused by the index asymmetry between the two waveguides. A minimum linewidth of 1.5nm is obtained.

Introduction: Wavelength division multiplexed (WDM) communication systems require narrow-band, wavelength stabilised, and fibre-coupled light sources. Traditionally, such devices are obtained with the use of diffraction gratings (written either on the semiconductor source or the fibre) and butt-coupling to fibres. This method leads to high fabrication costs and high insertion losses. An asymmetric waveguide coupler, which is made up of a semiconductor waveguide evanescently coupled to a singlemode fibre, can provide solutions to these problems. In this Letter, we describe a narrow-band light emitter, implemented with a polished fibre half coupler and a semiconductor anti-resonant reflective optical waveguide (ARROW).

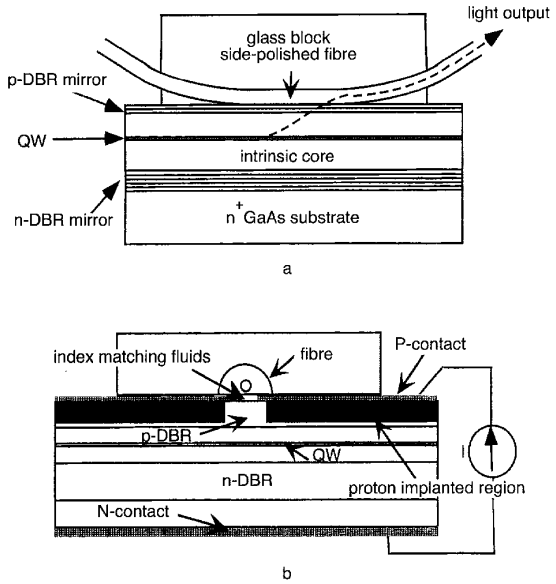

Fig. 1 *Schematic diagram of GaAsIAlGaAs in-line fibre light emitter*

a Side view
b Cross-sectional view
Proton implantation used to confine current injection to near fibre core

The fibre half coupler is made by epoxying a singlemode fibre into a curved groove in a glass substrate and then polishing both the substrate and the fibre cladding to within a few microns of the fibre core [1]. The ARROW consists of a core sandwiched between two distributed Bragg reflector (DBR) mirrors. The mirrors are doped to form a *pin* structure, and a quantum well is placed in the intrinsic region. When the ARROW is attached to the polished fibre half coupler, optical waves can be guided in its core by reflection from the *n*-doped DBR mirror on the one side, and a combination of reflection from the *p*-doped DBR mirror and total internal reflection from the fibre cladding on the other side. The device schematic is shown in Fig. 1. The mirrors help to support a propagating mode in the semiconductor that has a low enough effective index to phase-match to the fibre. The two waveguides have very different dispersion characteristics, therefore phase-matching occurs only at specific wavelengths. By forward biasing the *pin* diode, electrons and holes are injected into the intrinsic region and most of them recombine in the quantum well, creating photons. The photons are emitted into multiple modes, and only those that are phase-matched to the fibre mode are coupled into the fibre. Therefore, a narrow-band output from the fibre can be obtained.

Experiment: To demonstrate this device concept, a GaAs/AlGaAs ARROW was grown by molecular beam epitaxy (MBE) on an n^+ GaAs substrate. The *n*-type and *p*-type DBR mirrors consist of 40 and 5 pairs of AlAs/$Al_{0.33}Ga_{0.67}As$ quarter wave layers, respectively. The mirrors were optimised for maximum reflection at 25°, which is the mode angle required for phase-matching to the singlemode fibre. The *p*-type mirror was designed to be partially reflective so that there is sufficient field overlap between the guided modes of the fibre and the ARROW. The core of the ARROW was made up of an $Al_{0.33}Ga_{0.67}As$ layer and a 75Å GaAs quantum well. The quantum well was placed at the centre of the core where the intensity peak of the guided mode occurs.

Following MBE growth, the wafer was processed and cleaved into pieces for testing. During testing, the ARROW sample was mounted on a metal stage with conductive paste. A fibre half coupler (from Canadian Instrumentation and Research Ltd) with a polished interaction region of ~1mm in length was mounted on a *x-y-z* stage and positioned on top of the ARROW sample. The position of the fibre core was determined by launching light from a GaAs laser diode into the fibre half coupler and observing the scattered light with an infrared CCD camera. After aligning the fibre core to the ARROW, the two waveguides were brought into contact. Drops of index matching fluid, the index of refraction (1.458) of which was very close to the fibre cladding index (1.452), were applied at the interface to ensure good optical contact. The optical output from the fibre was observed using a spectrum analyser.

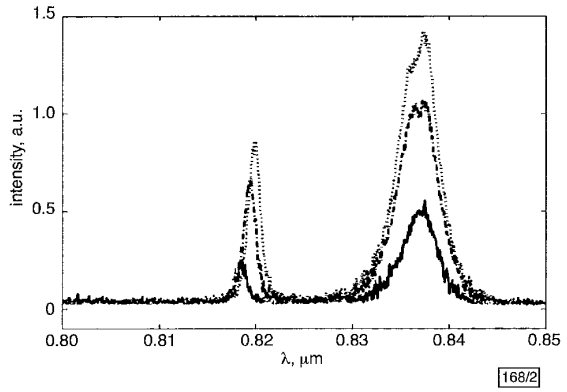

Fig 2 *Measured device emission spectra*

——— 40mA
–·–·– 80mA
····· 100mA

Results: The output spectra as a function of injection currents are shown in Fig. 2. The two groups of emission peaks correspond to TE and TM resonances. The TE (electric field vector parallel to the plane of the GaAs wafer) resonances have narrower linewidths mainly because of the higher reflectivity of the DBR mirrors, and hence lower ARROW propagation losses. There was no observed linewidth narrowing with increasing input current, which indicates that there were not sufficient carriers injected to produce transparency in the quantum well. The total output power measured with